Effect of temperature induced excess porewater pressures on the shaft bearing capacity of geothermal piles

Raul Fuentes [a,*], Nuria Pinyol [b], Eduardo Alonso [b]

[a] School of Civil Engineering, University of Leeds, Leeds, LS2 9JT, UK

[b] Department of Geotechnical Engineering and Geo-Sciences, Universidad Politecnica de Catalunya, c/ Jordi Girona, 1-3, Building D2, Barcelona, 08034, Spain

HIGHLIGHTS

- Geothermal piles in low permeability ($k < 1E{-}11$ m/s) and low compressibility clays ($K_S > 2E10$ Pa) can develop excess porewater pressures comparable to shaft friction.
- A shaft friction reduction ratio is presented to account for this.
- The solution presented provides an explanation to the difference between back-calculated and observed shaft frictions for a test pile.

ARTICLE INFO

ABSTRACT

Changes in temperature in clays of low permeability typically induce excess porewater pressures. In the context of geothermal piles this effect has typically been overlooked since most installations have occurred in soils with higher values of permeability. A parametric study is presented that solves the governing differential equations one dimensionally in a pile to study the influence of the various parameters: temperature of the fluid, permeability and soil compressibility. A new shaft resistance reduction ratio has been also defined to illustrate the loss of bearing capacity. The study shows that when the value of permeability is $1E{-}11$ m/s or lower, combined with a soil compressibility in excess of 20,000 MPa, the developed excess porewater pressures can potentially reduce the effective stress locally to very low values. The solution applied to the case of the Lambeth College, London, also provides a plausible explanation to the observed loss of shaft friction of the tested pile.

1. Introduction

Soils with low permeability can experience substantial increases in their porewater pressures as a consequence of temperature rises (e.g. Refs. 1–4).

Geothermal piles are used to exchange heat from the ground for heating and cooling of superstructures.[5] In their cooling mode, the temperature of the circulated fluid is higher than the soil's temperature; hence, increasing the temperature of the latter. Under normal operating conditions the fluid can be up to 30 °C, although greater temperatures have been tested (e.g. Refs. 5, 6). In low permeability soils, these temperature increases have the potential to increase the porewater pressures and reduce the available effective stress. If this reduction is in the same order as the mobilised shaft friction, their effect on the shaft resistance can be significant.

In order to study the full thermo-hydro-mechanical interaction between pile and soil, Laloui et al.[7] presented the complete formulation of the problem and a solution compared to a field test. The excess porewater pressures are included implicitly within the formulation but since the values of permeability reported in their case study were in the order to 10^{-6} m/s, no significant excess porewater pressures were observed and remained constant. In turn, this had little effect on the available shaft friction. However, in the presence of lower permeability soils, these excess porewater pressures can reach values in the order of 1 MPa for temperature increments of 30 °C,[3] which in most practical cases of bearing piles would exceed the effective stress at the interface. Bourne-Webb et al.[6] presented another pile test with temperature cycling where they reported a difference of 15 kPa between the back-analysed –
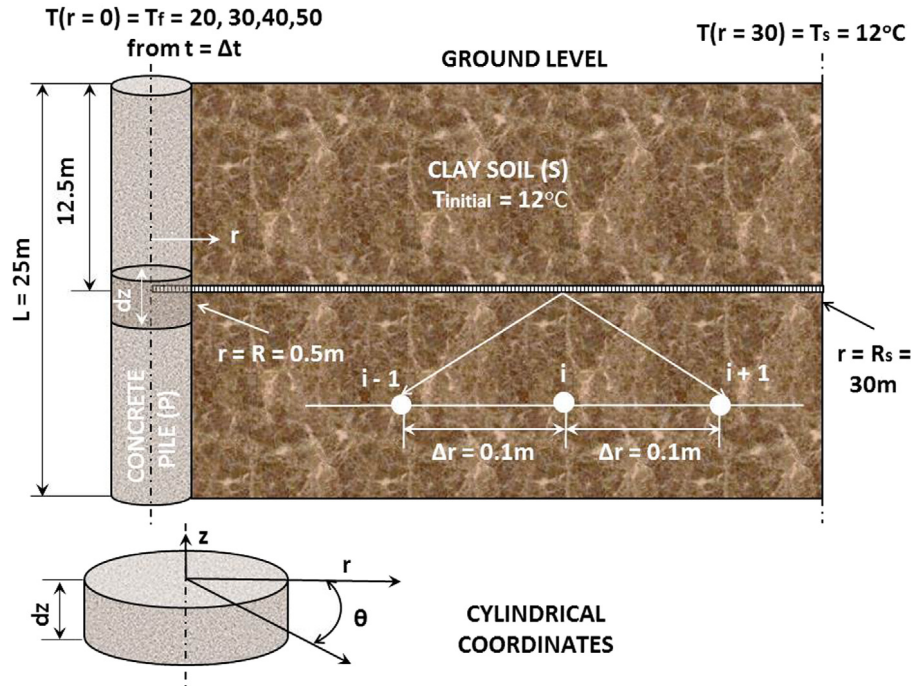
Fig. 1. Problem definition.

based on a mechanical test – shaft friction and the measured shaft friction as will be shown later in the paper.

Based on this evidence, this paper presents a finite difference solution to the fully coupled formulation to study the development of excess porewater pressures in geothermal piles and its impact on the shaft friction at the pile–soil interface. The emphasis will be on presenting comparisons in terms of orders of magnitude of excess porewater pressures and not attempting to specify accurately all properties as this will change from case to case. These comparisons do however, highlight an important issue that has been so far overlooked. The solution also provides a plausible explanation to the differences observed during the Lambeth College test presented in Ref. 6.

2. Problem definition, governing equations and assumptions

Fig. 1 shows the problem's geometry. A single pile diameter equal to 1 m and pile length of 25 m as used by Bourne-Webb et al.[6] were used. This length is enough to guarantee that seasonal effects are less important at mid-depth of the pile[8] where the comparison between methods is carried out.

The problem presents geometrical axisymmetry about the pile's axis so a cylindrical coordinate system (r, θ, z) was chosen as shown in Fig. 1. Additionally, Loveridge & Powrie[9,10] showed that the temperature difference at the pile surface for different positions within a pile diameter is lower than 2 ˚C: therefore, the azimuthal coordinate, θ, can be eliminated. Likewise, it is assumed that the temperature of the pile along its length is constant; this has been verified in site tests by multiple authors—e.g. Refs. 6, 7 for piles or Lee & Lam[11] for boreholes. This, combined with an assumption of fully hydrostatic initial porewater profile, allows eliminating the z coordinate as well. The problem then becomes one dimensional, defined in the radial direction, r. It must be noted that this assumption is more representative of points distant from the ground surface where the temperature of the soils is subject to variations from above-ground effects. Hence, the comparisons between calculation methods – explained later – were done at mid-depth of the pile as indicated in Fig. 1.

The thermo-hydro-mechanical formulation that defines the problem was presented generally by Olivella et al.,[12] and its application to piles by others like Laloui et al.[7] Both references present the full equations derivation and therefore, this paper only presents the final equations. For ease of reference, the reader is directed to Pinyol & Alonso[4] as the same nomenclature has been used here.

The heat equation for a constant thermal conductivity is

$$\frac{\partial T}{\partial t} = \alpha \frac{1}{r} \frac{\partial}{\partial r} \left(r \frac{\partial T}{\partial r} \right) = \alpha \left(\frac{1}{r} \frac{\partial T}{\partial r} + \frac{\partial^2 T}{\partial r^2} \right) \tag{1}$$

where the convection effects have been ignored as demonstrated by Laloui et al.[7] for values of permeability much higher than those covered here: hence, this assumption is even more applicable to our case.

The combination of soil and water mass balance formulations yields the final governing second order parabolic differential equation that applies only to the soil mass[4]

$$-\left[(1-n) \beta_s + \beta_w n \right] \frac{\partial T_s}{\partial t} + \left(n\alpha_w + \frac{1}{K_s} \right) \frac{\partial u}{\partial t}$$

$$-\frac{k}{\gamma_w} \frac{1}{r} \frac{\partial}{\partial r} \left(r \frac{\partial u}{\partial r} \right) = 0 \tag{2}$$

which has as unknowns the soil temperature, T_s, and the excess porewater pressures, u.

The main assumptions to derive the above equation are:

- The soil grains are incompressible against stress but not temperature changes.
- All the input variables – porosity, thermal conductivity, permeability, soil and water linear coefficients of thermal expansion, and soil and water compressibility – are independent of time, temperature and stress.
- The water table does not change throughout the test and therefore, in combination with small seepage forces due to low permeability, all changes to porewater pressures are due to the induced excess porewater pressures caused by thermal and mechanical strains.

Table 1
Parameter values for the parametric study.

Variable	Pile (C)	Soil particles (P)	Water (w)	Soil medium (S)
Porosity, n	–	–	–	0.25
Thermal expansion coefficient, β (1/°C)	–	3.00 E−05	3.42 E−04	1.10 E−04[a]
Compressibility constant, water, α_w (1/Pa)	–	–	5.00 E−10	–
Density, ρ (kg/m³)	2400	2700	1000	2275[a]
Thermal conductivity, Γ (W/m °C)	1.5	–	–	2.0
Specific heat, C (J/kg °C)	880.2	837.2	4186	1674.4[a]
Permeability, k (m/s)	–	–	–	1.00 E−8 1.00 E−9 1.00 E−10 1.00 E−11 1.00 E−12
Soil compressibility, K_S (Pa)	–	–	–	2.00 E06 2.00 E07 2.00 E08 2.00 E09 2.00 E10
Temperature of the fluid, T_f (°C)	20 30 40 50	–	–	–

[a] These variables were calculated using the rule of mixes—e.g. for density, $\rho_s = \rho_P (1 - n) + \rho_s n$.

- The soil volumetric deformation at the pile–soil interface can be characterised by a general one dimensional soil compressibility, K_S, as shown by Di Donna & Laloui.[13] The deformation caused in the pile due to temperature is therefore not included, similarly to what Hueckel et al.[14] analysed; however, authors like Olgun et al.[15] showed this deformation is negligible for undrained analysis of clays using a finite element model and a cavity expansion solution.
- The total horizontal stress at the pile–soil interface remains constant. It must be noted that Hueckel et al.[14] predicted a relative small horizontal total stress increment, compared to the porewater pressure, for a clay with a permeability of 1 E−12 m/s subject to temperature increments in the region of 15 °C at its interface with the heating element. Both values are the lowest and upper bounds respectively of those used in this paper. Hence, it is assumed that for greater permeabilities and lower temperatures like those used here, the assumption also holds. This assumption has also been confirmed by Olgun et al.[15] for undrained analysis of clays, which given the low permeability used here, it is highly applicable.
- The plastic, strength changes and long term effects at the pile–soil interface[16–19,8,20,13] that arise as a consequence of multiple heating and cooling cycles have been ignored. A single heating cycle is considered here.

Most variables in Eq. (2) are well defined and show little variation in the context of thermal piles. Hence, only those where variations in practice can be present were selected to undertake the parametric study. These are: permeability, k, soil compressibility, K_S, and the temperature of the fluid, T_f. The influence of each of the three parameters, provided all others are fixed, is conceptually known: higher fluid temperature or compressibility and lower permeability, all produce greater excess porewater pressures. It is its extent that is investigated hereafter.

Table 1 presents the different values that have been used for the parametric study. The fluid temperature has been taken within the typical ranges of operation for geothermal foundations.

The range of permeability values used include those typical of low permeability clays like London Clay,[21] Gault Clay,[22] Boom Clay,[23,24,14] or Opalinus Clay.[25] A maximum value of 1E−08 m/s was also used as an upper bound, beyond which Di Donna & Laloui[13] demonstrated that induced excess porewater pressures are of no concern.

3. Analysis

3.1. Finite difference (FD)

Eqs. (1) and (2) are uncoupled since the convective component caused by fluid movement affecting the temperature has been ignored. Hence, Eq. (1) can be solved and the results of this used as input into Eq. (2), which then turns into an equation where u is the only unknown.

3.1.1. Temperature field—Eq. (1)

The space domain was divided into three distinct stencils: within the pile, at the pile–soil interface, and within the soil. The discretisation was carried out using a regular grid size, Δr, of 0.0125 m—see Fig. 2.

Developing the energy balance for points within each material yields

$$\Gamma_i (r_i - \Delta r/2) \frac{T_{i-1} - T_i}{\Delta r} - \Gamma_i \left(r_i + \frac{\Delta r}{2} \right) \frac{T_i - T_{i+1}}{\Delta r}$$
$$= \rho_i C_i r_i \Delta r \frac{T_i' - T_i}{\Delta t} \qquad (3)$$

where the first term on the left hand side is the heat going into point i, Q_{i-}, and the second is the heat leaving point i, Q_{i+}—see Fig. 2(a). T_i' is the temperature in point i at the following time step. The right hand side of the equation is the heat generated in the vicinity of point i due to temperature changes in time. The equation can be rearranged to isolate T_i' as

$$T_i' = T_i + \alpha_i \frac{\Delta t}{r_i \Delta r^2} \left[\left(r_i - \frac{\Delta r}{2} \right) (T_{i-1} - T_i) \right.$$
$$\left. - \left(r_i + \frac{\Delta r}{2} \right) (T_i - T_{i+1}) \right]. \qquad (4)$$

At the pile–soil interface, the problem involves both materials—see Fig. 2(b). The energy balance is as follows

$$\Gamma_c (R - \Delta r/2) \frac{T_{R-1} - T_R}{\Delta r} - \Gamma_s \left(R + \frac{\Delta r}{2} \right) \frac{T_R - T_{i+1}}{\Delta r}$$
$$= (\rho_c C_c (R - \Delta r/4) + \rho_s C_s (R + \Delta r/4)) \frac{\Delta r}{2} \frac{T_R' - T_R}{\Delta t} \qquad (5)$$

(a) Within each material, i.

(b) Interface pile–soil.

(c) Adjacent to concrete pile central axis after the first time increment.
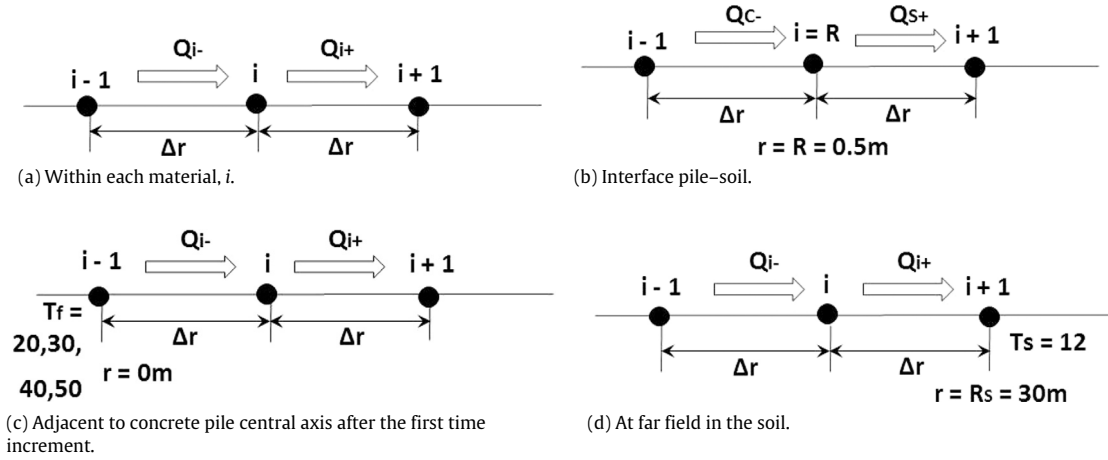
(d) At far field in the soil.

Fig. 2. Finite different discretisation stencils.

where T_R' is the temperature at the interface in the following time step. The terms are similar to those in Eq. (3). However, now the two different materials affect both the left and right hand sides of the equations. Q_{i-} is Q_{c-} (within the concrete pile), and Q_{i+} is Q_{S+} (within the soil)—see Fig. 2(b).

T_R' can be then isolated as

$$T_R' = T_R + \frac{2\Delta t}{\Delta r^2} \frac{1}{\left(\rho_c C_c \left(R - \Delta r/4 \right) + \rho_s C_s \left(R + \Delta r/4 \right) \right)}$$

$$\times \left[\Gamma_c \left(R - \frac{\Delta r}{2} \right) (T_{R-1} - T_R) \right.$$

$$\left. - \Gamma_s \left(R + \frac{\Delta r}{2} \right) (T_R - T_{R+1}) \right]. \tag{6}$$

Two Dirichlet boundary conditions are used

$$T(r = 0) = T_f \tag{7}$$

and

$$T(r = R_s) = T_s \quad \text{for any time, } t. \tag{8}$$

The initial conditions are constant temperature everywhere and equal to that of the soil

$$T = T_S \quad \text{for all points.} \tag{9}$$

In the first time increment, the temperature at the pile axis is then instantly increased to the fluid temperature—see Fig. 2(c).

The equation was solved explicitly in the time domain. An initial estimate of the maximum time step was calculated using the Neumann criteria for parabolic differential equations. For Eq. (1), this means

$$\Delta t_1 = \frac{\Delta r^2}{2\alpha_C}. \tag{10}$$

The consistency and stability of the solution was checked by using one order of magnitude lower than the calculated time step: if both yielded the same result, the solution was accepted. Similarly, its independence to the space discretisation was also carried out until no further discretisation improved the results.

3.1.2. Excess porewater pressures field (soil only)—Eq. (2)

Making

$$K_1 = -[(1 - n)\beta_s + \beta_w n] \tag{11}$$

$$K_2 = \left(n\alpha_w + \frac{1}{K_s} \right) \tag{12}$$

$$K_3 = -\frac{k}{\gamma_w} \tag{13}$$

allows rewriting Eq. (2) as

$$K_1 \frac{\partial T_s}{\partial t} + K_2 \frac{\partial u}{\partial t} + K_3 \frac{1}{r} \frac{\partial}{\partial r} \left(r \frac{\partial u}{\partial r} \right) = 0. \tag{14}$$

The above equation was solved using the solver-function: "pdepe" – and the ordinary differential equation solver-function: "ode15s" – in MATLAB (version R2013b-8.2.0.701). A combination of Neumann,

$$\left(\frac{\partial u}{\partial r} \right)_{r=R} = 0 \quad \text{for any time, } t \tag{15}$$

indicating that there is no flow at the pile–soil interface, and Dirichlet boundary conditions

$$u(r = R_s) = 0 \quad \text{for any time, } t \tag{16}$$

that shows there is no excess porewater pressure generated in the far field, were used.

The initial conditions are zero excess porewater pressures

$$u(t = 0) = 0 \text{ throughout} \tag{17}$$

as it assumes a hydrostatic porewater pressure profile.

4. Results and discussion

Fig. 3 shows the different temperature profiles at the pile–soil interface evolving with time. Each of the FD solutions for the different temperatures used converges towards steady-state values, that were verified by calculating the steady state temperature obtained from Eq. (1) when removing the time dependent term with the same boundary and initial conditions.

Fig. 4 shows the results of 100 models resulting from the combinations of T_f, k and K_s values shown in Table 1. As expected, lower permeability produces greater porewater pressures, as does a less compressible soil at the interface and, obviously, higher temperature. For the most detrimental combinations, the porewater pressure values reach over 0.2 MPa, which is substantially higher than the available horizontal stress for typical geothermal piles.

Interestingly, increases of one order of magnitude in K_s (Fig. 4(a)) result in much greater relative increments of excess porewater pressures than an order of magnitude decrement in permeability (Fig. 4(b)). This shows the importance of the soil stiffness and is shown by the greater slope in the $K_s - u$ plane in Fig. 4.
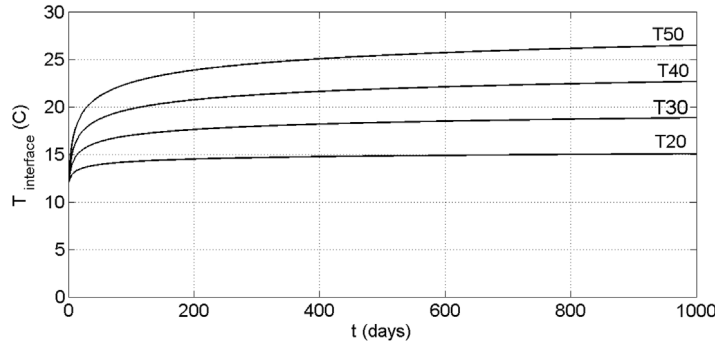
Fig. 3. Temperature at the pile–soil interface vs. time for the T_f values provided in Table 1.
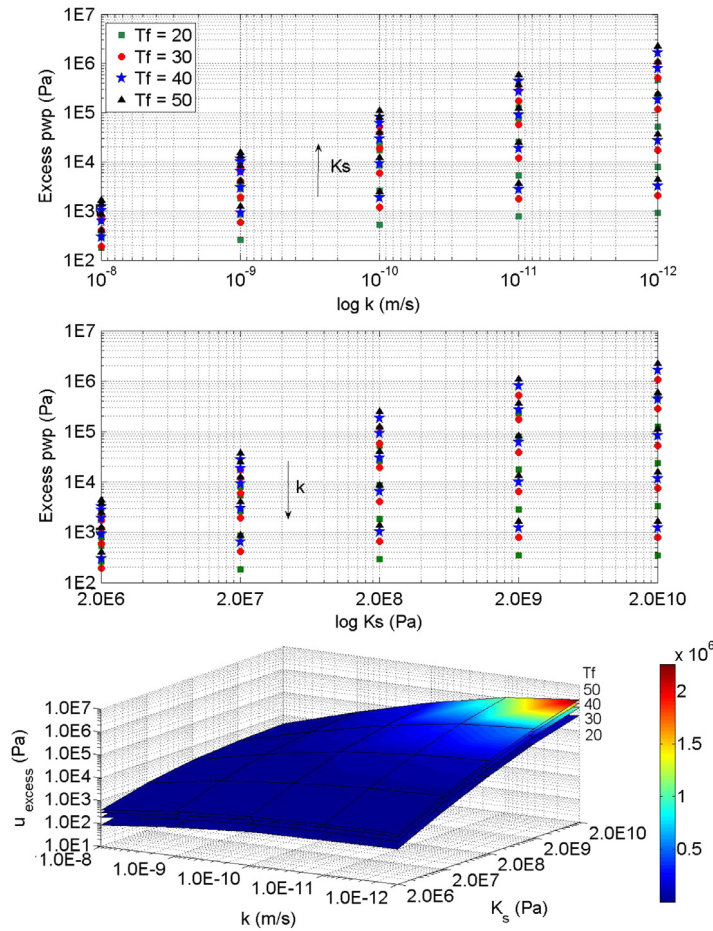

Fig. 4. Calculated excess porewater pressures against: (a) Permeability, (b) soil interface compressibility and (c) permeability and soil interface compressibility—all axes are in logarithmic scale.

4.1. Shaft resistance reduction ratio

The importance of the presented induced excess porewater pressures can be expressed as a *shaft resistance reduction ratio* defined as

$$R_\tau = \frac{\tau_{w/temp}}{\tau_{wo/temp}} \tag{18}$$

where $\tau_{w/temp}$ is the shear at the pile–soil interface with temperature changes and $\tau_{wo/temp}$ without temperature.

But the shear at the interface can be generally written as

$$\tau = \sigma'_h \tan \varphi'$$

which can be developed into

$$\tau = K_m \sigma'_v \tan \varphi' \tag{19}$$

by using a mobilised earth pressure coefficient at the interface, K_m. Writing the vertical effective stress as a function of total and porewater pressures for the case with temperature gives

$$\tau_{w/temp} = K_m (\sigma_v - u_o - \Delta u) \tan \varphi' \tag{20}$$

where u_0 is the initial porewater pressure before temperature changes are applied, and Δu is the induced excess porewater pressure from temperature changes. The same can be done for the case without temperature as

$$\tau_{wo/temp} = K_m (\sigma_v - u_o) \tan \varphi'. \tag{21}$$

Substituting Eqs. (20) and (21) into (18), and assuming that K_m and $\tan \varphi'$ do not change when the temperature gradient is applied,
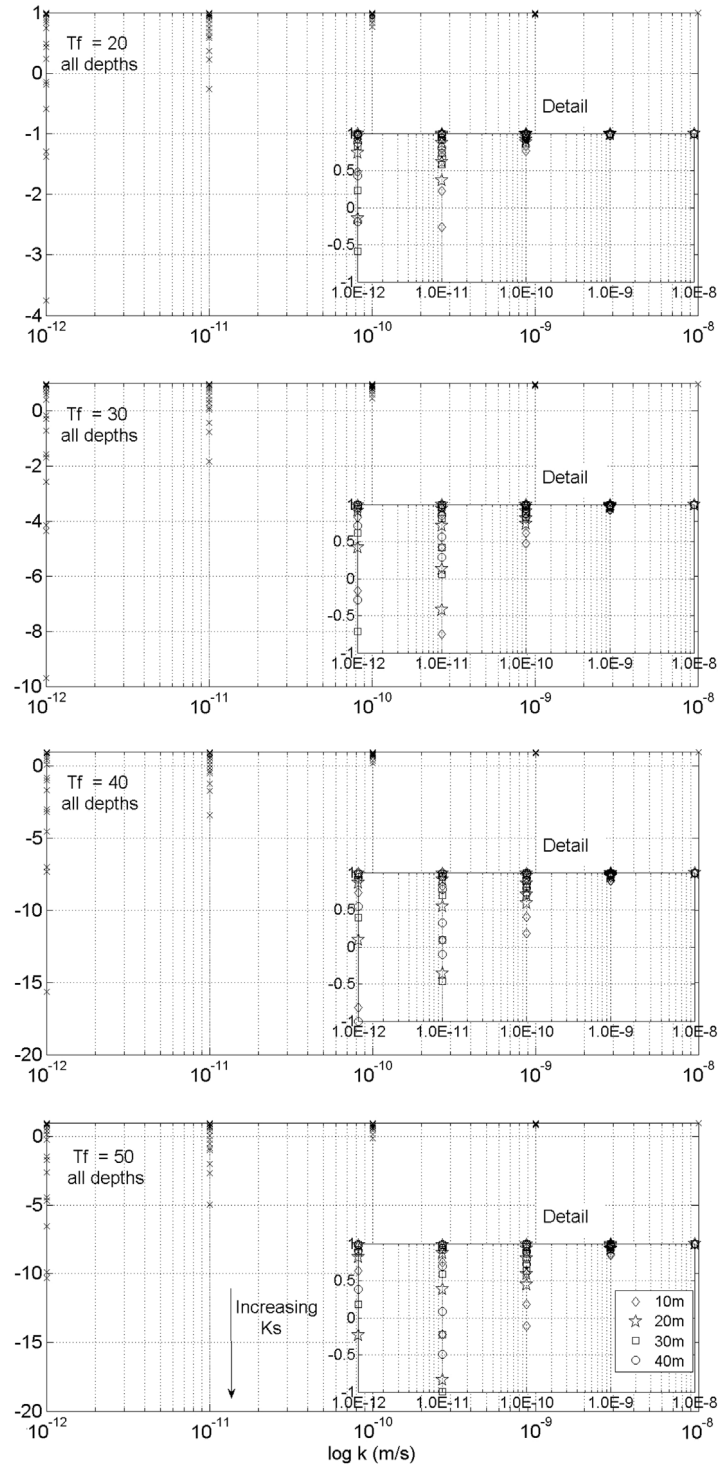
Fig. 5. Shaft resistance reduction ratio vs. permeability for different fluid temperatures: (a) 20 °C, (b) 30 °C, (c) 40 °C, (d) 50 °C.

gives the most general form of the shaft resistance reduction ratio

$$R_\tau = \frac{\sigma_v - u_o - \Delta u}{\sigma_v - u_o} \tag{22}$$

or

$$R_\tau = 1 - \frac{\Delta u}{\sigma_v - u_o}. \tag{23}$$

The independence of K_m and $\tan \varphi'$ to temperature gradients was shown by Di Donna & Laloui[13] who showed that the strain

and total stress changes at the interface are small when the temperature is applied.

The ratio R_τ, is equal to 1.0 when there is no heat (i.e. $\Delta u = 0$), 0 if $\Delta u = \sigma_v - u_0$, and negative when $\Delta u > \sigma_v - u_0$, or in other words, when the excess porewater pressure is greater than the initial vertical effective stress.

For saturated soils where the water table is at the ground surface and the vertical planes are principal planes[14], $\sigma_v = \gamma_{sat} z$ and $\gamma_{sat} z - u_0 = \gamma' z$, Eq. (22) can be rewritten as

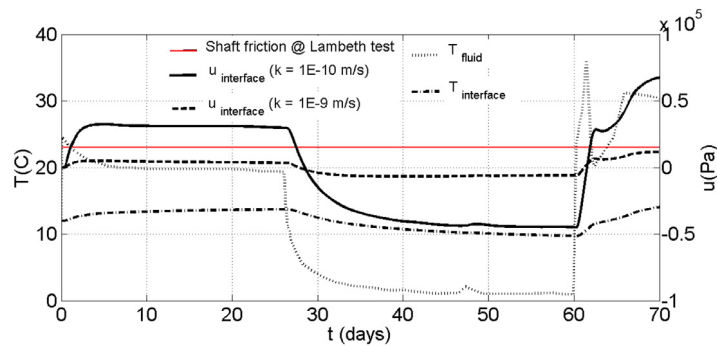$$R_\tau = 1 - \frac{\Delta u}{\gamma' z}. \tag{24}$$

Fig. 6. Temperature and excess porewater pressures for the Lambeth College case study.

Similarly to Eq. (22), the ratio is equal to 1.0 when there is no heat (i.e. $\Delta u = 0$), 0 if $\Delta u = \gamma' z$, and negative when $\Delta u > \gamma' z$.

For the purpose of this paper, it was assumed that the datum of z and the hydrostatic water table are at ground level for simplicity. Based on this, we present the results at 10, 20, 30 and 40 m depths and the same combinations from Table 1 as previously, in Fig. 5. It shows that, as expected, the deeper the evaluation depth along the pile, the more safety is present. It also shows that for values of permeability lower than 1.00 E−11 (m/s) and soil compressibility above 2E10 (Pa), the excess porewater pressures exceed the available shaft resistance regardless of the depth—i.e. R_τ is lower than 0. This highlights the importance of both values of k and K_s. Whilst the temperature of the fluid has an influence, this is much lower comparatively.

5. Lambeth College test[6] comparison

Fig. 6 shows the results of the proposed semi-analytical FD solution to the case study of a test pile in London Clay presented by Bourne-Webb et al.[6]. For the modelling, the temperature of the fluid, T_f, was taken as the temperature measurements in the pile presented by the authors. Values of permeability of 1E−9 m/s and 1E−10 m/s and soil compressibility equal to 3.71E10 Pa were taken from typical values presented by Hight et al.[21] for London Clay, as site specific measurements were not available.

The results in Fig. 6 show that the temperature at the interface experiences small increments compared to the previous cases where the fluid temperature was sustained. Despite, the much lower values, it still shows an effect on the excess porewater pressures reaching values of 4 kPa and 31 kPa at the end of the first heating cycle for both values of permeability used. These values are comparable and provide upper and lower bounds to the unaccounted difference of 15 kPa between the measured shaft friction and the ultimate shaft friction measured in the pile test Bourne-Webb et al.[6] reported. It therefore, provides a plausible explanation to this difference showing the effect of temperature on shaft friction.

6. Conclusions

The temperature induced excess porewater pressures in low permeability clays adjacent to thermal piles can be significant. Values in excess of 0.2 MPa have been proven in this paper under the assumption of constant total horizontal stresses at the pile–soil interface.

Soil permeability and soil compressibility are the most influential variables affecting the development of excess porewater pressures. In general, the lower the permeability, the greater the porewater pressure will be. Equally, for lower values of permeability the effect of the soil compressibility is accentuated, whereas in higher values of permeability, this is less relevant with regard to porewater pressures.

A new ratio named *shaft resistance reduction ratio* has been defined. It allows calculating, on a case by case basis, the potential for the developed porewater pressures to be of concern in terms of the shaft bearing capacity of thermal piles.

The parametric study has shown that only when the value of permeability is 1E−11 m/s or lower, combined with a soil compressibility in excess of 2E10 Pa, the excess porewater pressures were problematic. This combination of values of k and K_s is however characteristic of many overconsolidated clays.

The solution applied to the case of a test pile in London Clay, an overconsolidated clay, using typical values has provided a plausible explanation to the loss of shaft friction that was reported by Bourne-Webb et al.[6].

The results shown have significant implications for the design and operation of geothermal piles installed in low permeability and low compressibility soils and therefore, deserves further study from the community: the authors hope this paper will incentivise this. These effects are especially relevant in schemes were the ground is used as a heat sink for cooling during sustained periods of time. In more typical installations comprising heating and cooling cycles, the effect is smaller, but could also be comparably significant in relation to shaft friction resistance if the soil's permeability is very low.

Future work will focus on studying of the effect presented here with a more accurate pile–soil interaction modelling capable of modelling the plastic and long term deformations, concrete cracking, pile installation effects, and varying parameters with temperature and stress such as permeability and porosity.

Appendix A. Supplementary material

Supplementary material related to this article can be found online at http://dx.doi.org/10.1016/j.gete.2016.10.003.

References

1. Laloui L. Thermo-mechanical behaviour of soils. *Rev Fr Civ*. 2001;5(6):809–843.
2. Vardoulakis I. Dynamic thermo-poro-mechanical analysis of catastrophic landslides. *Geotechnique*. 2002;52(3):157–171.

3. Munoz JJ. *Thermo-hydro-mechanical analysis of soft rock application to large scale heating and ventilation tests* Doctoral thesis, Barcelona: Universitat Politecnica de Catalunya; 2007.

4. Pinyol NM, Alonso EE. Fast planar slides. A closed-form thermo-hydro-mechanical solution. *Int J Numer Anal Methods Geomech*. 2010;34(1):27–52.

5. Brandl H. Energy foundations and other thermo-active ground structures. *Geotechnique*. 2006;56(2):81–122.

6. Bourne-Webb PJ, Amatya B, Soga K, Amis T, Davidson C, Payne P. Energy pile test at lambeth college, London: Geotechnical and thermodynamic aspects of pile response to heat cycles. *Geotechnique*. 2009;59(3):237–248.

7. Laloui L, Nuth M, Vulliet L. Experimental and numerical investigations of the behaviour of a heat exchanger pile. *Int J Numer Anal Meth Geomech*. 2006;30: 763–781.

8. Pasten C, Santamarina JC. Thermally induced long term displacement of thermoactive piles. *J Geotech Geoenviron Eng*. 2014;140(5):06014003.

9. Loveridge F, Powrie W. Pile heat exchangers: Thermal behaviour and interactions, (2013). *Proc Inst Civ Eng: Geotech Eng*. 2013;166(2):178–196.

10. Loveridge F, Powrie W. 2D thermal resistance of pile heat exchangers. *Geothermics*. 2014;50:122–135.

11. Lee CK, Lam HN. Computer simulation of borehole ground heat exchangers for geothermal heat pump systems. *Renew Energy*. 2008;33:1286–1296.

12. Olivella S, Gens A, Carrera J, Alonso EE. Numerical formulation for a simulator (CODE_BRIGHT) for the coupled analysis of saline media. *Eng Comput*. 1996; 13(7):87–112.

13. Di Donna A, Laloui L. Numerical analysis of the geotechnical behaviour of energy piles. *Int J Numer Anal Meth Geomech*. 2014;39:861–888.

14. Hueckel T, Francois B, Laloui L. Temperature-dependent internal friction of clay in a cylindrical heat source problem. *Geotechnique*. 2011;61(10):831–844.

15. Olgun CG, Ozudogru TY, Arson CF. Thermo-mechanical radial expansion of heat exchanger piles and possible effects on contact pressures at pile–soil interface. *Geotech Lett*. 2014;4:170–178.

16. Di Donna A, Ferrari A, Laloui L. Experimental investigations of the soil–concrete interface: physical mechanisms, cyclic mobilization, and behaviour at different temperatures. *Can Geotech J*. 2015;53(4):659–672.

17. Yavari N, Tang AM, Pereira JM, Hassen G. Effect of temperature on the shear strength of soils and the soil–structure interface. *Can Geotech J*. 2016;53(7): 1186–1194.

18. Akrouch GA, Sanchez M, Briaud J. Thermomechanical behavior of energy piles in high plasticity clays. *Acta Geotech*. 2014;9(3):1–14.

19. Ng CWW, Shi C, Gunawan A, Laloui L. Centrifuge modelling of energy piles subjected to heating and cooling cycles in clay. *Geotech Lett*. 2014;4:310–316.

20. Stewart MA, McCartney JS. Centrifuge modeling of soil–structure interaction in energy foundations. *J Geotech Geoenviron Eng*. 2014;140(4).

21. Hight DW, Gasparre A, Nishimura S, Minh NA, Jardine RJ, Coop MR. Characteristics of the London clay from the terminal 5 site at heathrow airport. *Geotechnique*. 2007;57(1):3–18.

22. Ratman S, Soga K, Whittle RW. A field permeability measurement technique using a conventional self-boring pressuremeter. *Geotechnique*. 2005;55(7): 527–537.

23. Horsemann ST, Winter MG, Entwistle DC. Geotechnical characterization of boom clay in relation to the disposal of radioactive waste. *Comm Eur*. 1987.

24. Francois B, Laloui L, Laurent C. Thermo-hydro-mechanical simulation of ATLAS in-situ large scale test in boom clay. *Comput Geotech*. 2009;36(4):626–640.

25. Thury M, Boisson JY, Bossar P. Le laboratoire souterrain du Mont Terri (Suisse) et premiers résultats des études hydrogéologiques d'une formation argileuse. *Hydrogeologie*. 2000;2:13–22.